

Low energy cluster impact simulated by molecular dynamics; angular distribution of sputtering yield and impact under various impact angles

K. Barghorn* and E.R. Hilf

Department of Physics, Carl v. Ossietzky-University Oldenburg, D-26111 Oldenburg, PO Box 2503, Germany

The collision process of low energetic gold atoms and solid targets has been simulated using our molecular dynamics simulation code CLIMPACT II. The used algorithm is a third-order predictor Verlet algorithm [L. Verlet, Phys. Rev. 159 (1967) 98; W.F. van Gusteren and H.J.C. Berendsen, in: *Molecular Liquids – Dynamics and Interfaces*, A.J. Barnes et al., eds. (Reidel, 1984) p. 475.]. The iteration time step is continuously optimized by the program. About 50% of the total computer time is spent to integrate the motions during the first 100 fs of simulation time [B. Nitzschmann, Diploma thesis, Univ. of Oldenburg, Germany, 1992]. When the crater formation ends and the motions in the target are slower, the step increases up to 20 times the start step size. Using this algorithm we are able to simulate a target of up to 10^5 particles. We use new nonreflecting boundary conditions. Only mechanical interactions are considered. The projectile can be chosen as a cluster with variable impact angle. Specifically the output yield under different impact angles and the distribution of the desorbed particles are presented and discussed. The temporal development of the desorption shows three distinct processes: an early explosive process, a surface ablation by an apparent surface shock wave, a final thermal evaporation.

1. Introduction

For better understanding of cluster-impact-processes we developed a new molecular dynamics program CLIMPACT II [3]. The main intention was to simulate the impact of nonmolecular clusters into non-molecular solids.

This code is able to handle systems of up to 10^5 neutral particles with a total impact energy of the incoming projectile of up to 10 keV. Codes have been developed for deposition processes by other groups [4–7] as well. The velocities of the particles there are usually much slower by using lower impact energies. Tombrello and Shapiro [8] use a code for simulation of an impact of systems of up to 5000 particles.

In our simulations the target will still be intact after 10 ps, by using new boundary conditions which drain energy from the system. A crater will remain. It is good for crater studies and also for calculating yields of desorbed particles. We are able to track the trajectory of the impacting cluster atoms as well as the desorbed atoms and clusters.

The behaviour of the target and the projectile is recorded in data files. A 2-dimensional movie will help

to understand the process by visualizing the temporal development of the sputtering.

2. Iteration code and preparation

For simulations of large systems (in our case more than 40 000 particles) it was necessary to develop and use a fast code. This is assured by employing a third order Verlet algorithm:

$$r_i(t+h) = 2r_i(t) - r_i(t-h) + h^2 a_i(r_i(t)) + O(h^4),$$

$$a_i = -\nabla_i U_i(r^N).$$

For large systems of N particles, up to $N(N-1)/2$ interactions may occur. In molecular dynamics calculations with more than 10^4 particles it is common to define spatial grids where the particles are sorted into the blocks according to their current positions. So for the interaction between particles only neighbours of surrounding grid blocks have to be considered. The cutoff radii for primary and secondary next neighbours are $r_{c_n} = 1.1\sigma$ and $r_{c_t} = 2.5\sigma$ (σ is the fcc lattice constant).

The primary neighbours are ten times more often iterated than secondary neighbours. So the cutoff corresponds to the secondary next neighbours.

* Corresponding author.

The most widely used and fastest algorithm, the neighbour link-list algorithm by Hockney and Eastwood [9] was used.

2.1. Energy conservation

Conservation laws such as for the total energy are not automatically fulfilled by MD calculation codes. The Verlet algorithm is not as accurate as higher order Gear methods [5,10], but we are interested in making the timestep δt as large as possible. With longer timesteps, the Verlet algorithm is more attractive [11]. The root-mean-square energy fluctuation $\langle \delta H \rangle^{1/2}$ is closely proportional to δt^2 for the Verlet algorithm, but for other higher order methods worsens much more rapidly with increasing δt [12].

An automatical generator for the size of the timesteps was prepared [3]. The stepsize varies from 0.01 up to 5 fs.

The code ensures that the timestep does not become so large that the atoms can move more than a small fraction of the lattice constant by a timestep adjustment. The program takes the current velocities to determine the timestep for the next iteration step, the accelerations do not change more than a fraction of one order of magnitude. We are working on tracking the total energy with iteration time to test the quality of the code.

2.2. Target preparation

The desorption process has been simulated by means of a 3D-molecular dynamic computer simulation of a

collision between a 3-atom gold cluster and a monocrystal gold target of $24 \times 24 \times 18$ elemental cells ($\approx 40\,000$ particles) with an (in our case) fcc structure and cubic proportions prepared with the Lennard–Jones potential for the interatomic interactions as a simplest test case. The parameter $\sigma = 1.88 \text{ \AA}$ and $\epsilon = 0.2 \text{ eV}$ have been determined by the formula given in ref. [13], where only twelve next neighbours are considered.

Other authors have tried to develop more realistic potentials like combinations between pair potentials e.g. Morse and Molière [14] or embedded atom potentials [4].

The differences between EAM and pair potentials are explored by Tombrello [15].

2.3. Boundary condition

One necessary condition for the simulation of large systems is the choice of a suitable boundary condition.

With free borders it is impossible to simulate cluster impact processes. A target of less than 5000 particles will be destroyed by an incoming projectile with more than 1 keV total energy well before the real desorption process stops.

Others use a hard border to fix the target. The effect is a thermal sputtering of all free particles. The shock wave will be totally reflected at the border. So the simulation must be stopped before the shock wave reaches the border.

A way out is to drain energy from the system. Different possibilities are proposed. Tombrello et al.

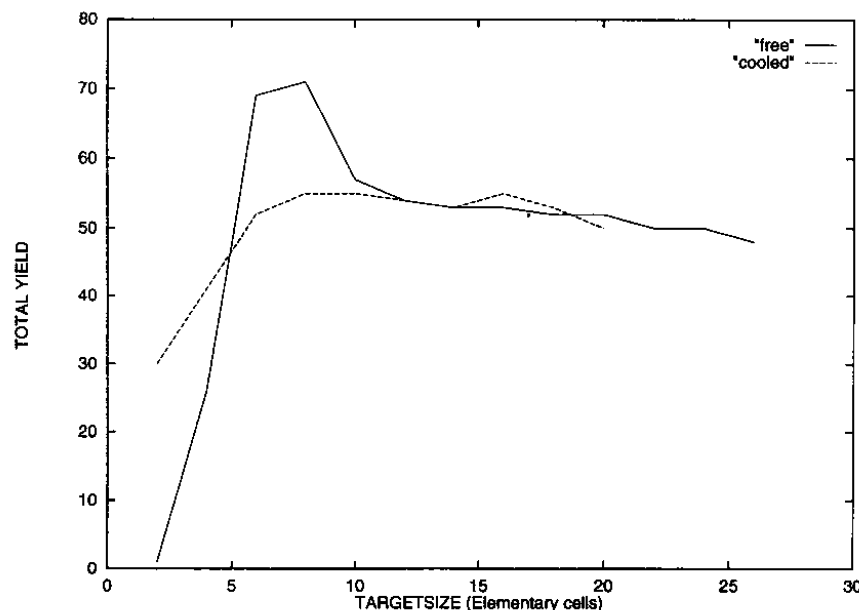


Fig. 1. Total yield versus target size under different boundary conditions. The dotted line shows the behaviour for free borders, the solid line under our damping boundary conditions.

[16] use a damped restoring force of the form $F_R = -m\omega^2 - r - m\sigma v$, for a single layer of atoms on the sides and the back of the target. Haberland [4] uses a separation of border atoms into a damped area and a fixed area.

The problem is to minimize the reflection of the shock wave at the border and to minimize the loss of particles at the border.

Therefore we introduced a region around each tar-

get (except the surface) of size $3r_0$, where an additional force $F_{x,y,z} = -\alpha v_{x,y,z}^\beta$ is applied to each particle. α and β have been determined by simulating a 1-dimensional linear chain, optimizing the damping for minimum momentum reflection. The parameters were set as $\alpha = 1100$ amu and $\beta = 2$. It was found that the nonlocality of this friction function force is necessary to minimize the momentum reflection [3].

This was tested for very low impact energies of 0.5

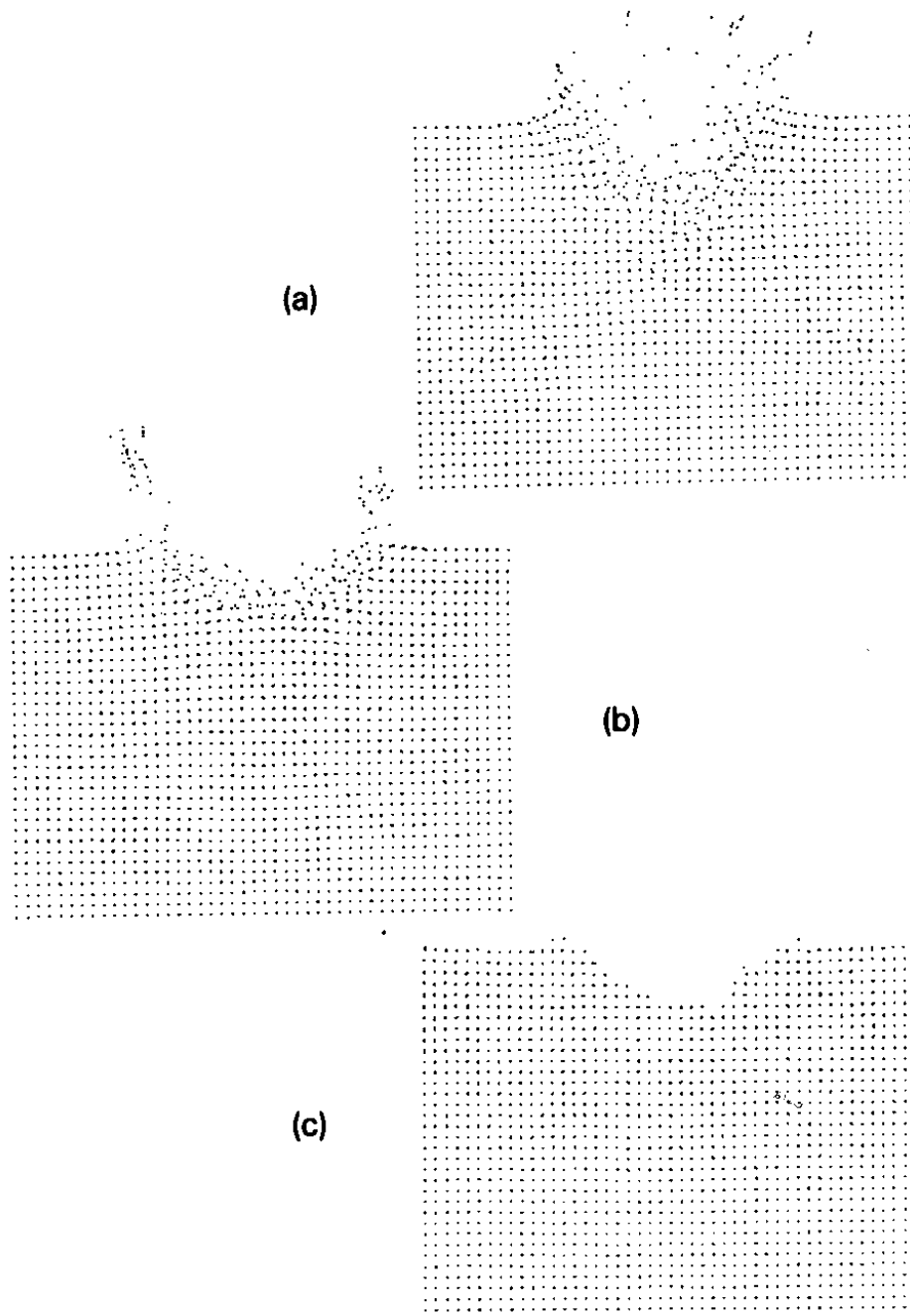


Fig. 2. Spots from the 2-D movie. It shows an impact of a 3 Au cluster into a fcc Au target. The total impact energy was 3 keV, the impact angle 70° . (a) Simulation after 1.5 ps, (b) after 3.3 ps, (c) after 10 ps.

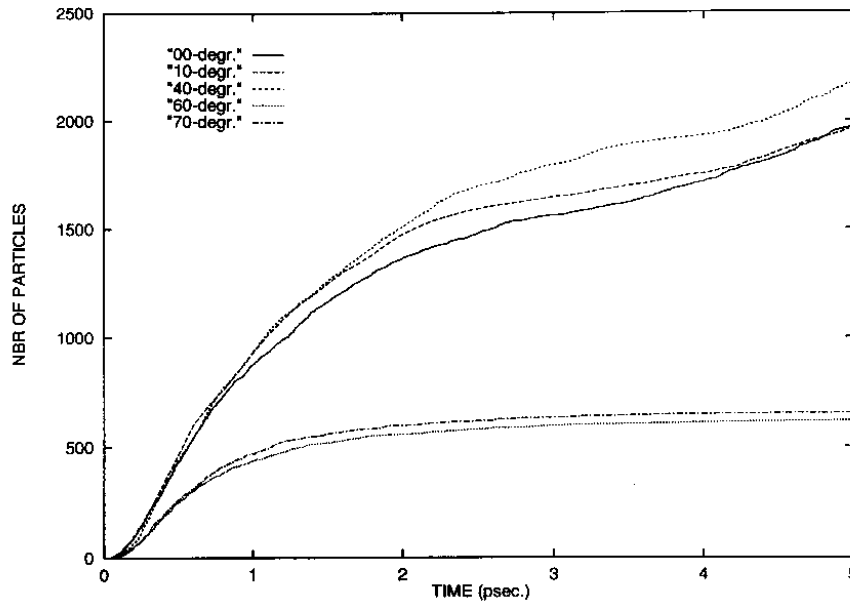


Fig. 3. Total yield for various impact angles versus the iteration time. It shows the dependence of the impact angle.

keV per atom (see Fig. 1). The plot shows the total yield versus target sizes. The dotted line (free boundary conditions) reaches a fixed value for the total yield later than total yields under damped boundary conditions.

The free boundary condition gives 40% too high total yield if the target is too small. Thus free boundary conditions calculations need larger targets to achieve the same accuracy for the results.

This qualitative new finding applies to any atomic force chosen.

The boundary condition choice is important, even for the largest grid computational calculatable at present (10^4 - 10^5 particles), because the desorption still takes place when the shock wave reaches the border. Since the experimental yield data are just the total time integrated desorption yield, the whole time span has to be followed by simulation, not just the very early part,

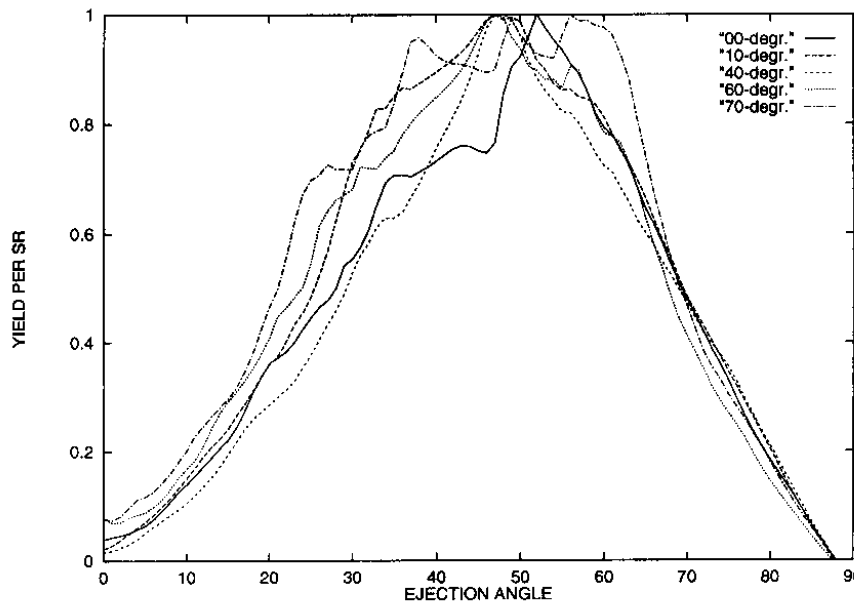


Fig. 4. Angular distribution of ejected particles under various impact angles. The plot shows the number of sputtered particles per steradian normed to the maximum of each distribution.

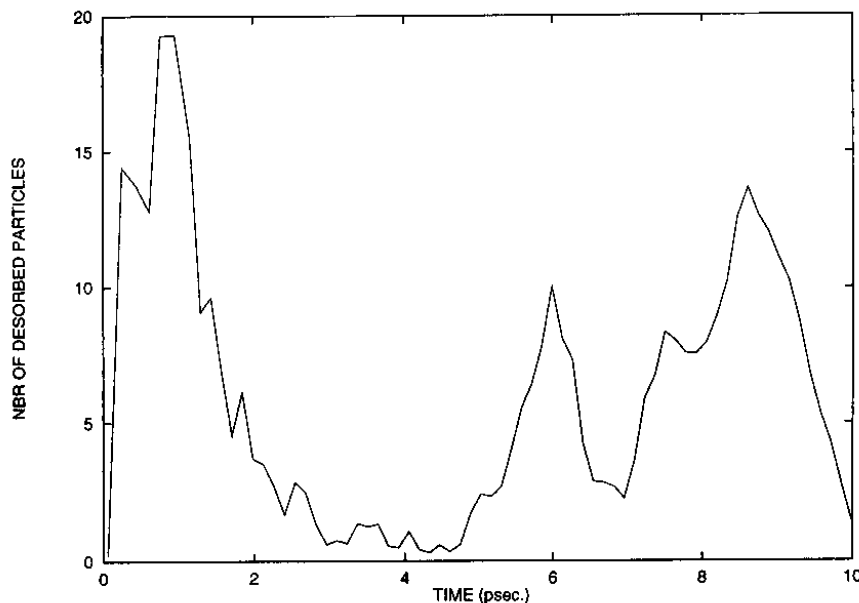


Fig. 5. Temporal development of the desorption. Plotted is the number of sputtered particles per timestep versus the iteration time. This example is from an impact angle of 70° , see Fig. 2.

where the boundary condition chosen would not yet enter.

In Fig. 5 this is the case for about 2 ps, whereas desorption continues up to 10 ps. Thus a momentum nonreflecting boundary condition is absolutely compulsory.

2.4. Simulation preparation

The projectile particles (a cluster of 3 Au atoms) are placed above the target top with a velocity of 300

$\text{\AA}/\text{ps}$ towards the target center under various impact angles. When hitting the target, some projectile particles are reflected, others penetrate, but both initiate a shock wave which propagates towards the target boundary.

A 2-dimensional movie of the 3-dimensional simulation is created by the program. It shows a cut through the target including the impact track (see Figs. 2a–2c). The figures are taken from the simulation series of varying impact angles (here 70°). A series of various impact angles were simulated.

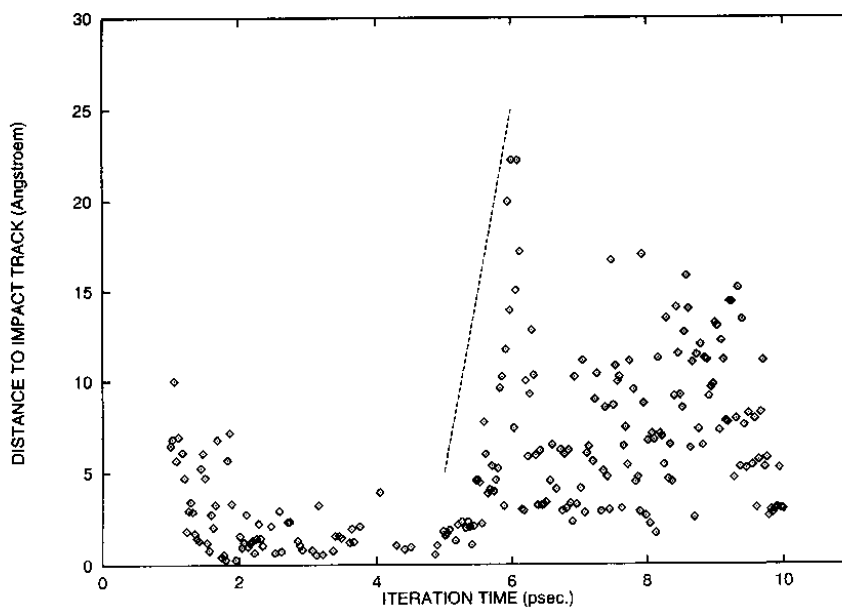


Fig. 6. A distribution of particle ablation. It shows the iteration time versus the distance of ablating to the impact track. The dotted line shows the sound velocity in gold. It is also taken from the 70° impact.

The presented data are individual shoots. For the small number of atoms in the projectile cluster fired on an fcc-lattice there might be some slight orientation bias, especially in the off-scattering plane. However, the main part of the process is statistically extremely violent (many collisions) and thus the original information on the exact original lattice positions is quickly lost.

3. Results

3.1. Dependence of total yield on impact angle

We found that the total yield of sputtered particles depends on the impact angle of the projectile. The maximum of the yield is not given under an impact angle perpendicular (0°) to the target surface. However, it is at a magic angle at $\approx 40^\circ$ (Fig. 3).

3.2. Angular distributions of sputtering particles

The angular distribution of sputtering yield does not depend on the impact angle (see Fig. 4). For all impact angles the angular distribution of ejected particles is very similar. This result was taken from the same simulation series as above.

3.3. Temporal development of desorption process

The result was taken by an impact of three gold atoms into a gold target. The impact energy was 3 keV totally. The impact angle was 70° .

In Fig. 5 we plotted the temporal development of the desorption. The first phase of desorption starts soon after the impact. The explosive desorption of particles is close to the impact track (see Fig. 6). So we conclude that this is an explosive process which reaches its maximum after 1 ps. The projectile transmitted its total energy. After 3 ps the explosion process ends. At 5 ps we got a new separate effect at the surface, the ablation of the particles by a radially emitted transversal nonlocal surface shock pulse (surface soliton) is consistently good all over the surface (see Fig. 6).

This effect of surface ablation is in good agreement with recent macroscopic calculations by Barth [17]. The desorption process ends with a statistical sputtering period (thermal evaporation) starting at about 7 ps. The statistical sputtering of particles occurs not all over the surface but just in the neighbourhood of the impact track. Thus, we conclude that it is a thermal effect. After 10 ps the process is nearly over and a target near thermal equilibrium but with a crater remains. Work with different target sizes is in progress to

confirm that the three maxima are not due to the return of energy and momentum for desorption after reflection at the boundaries. In Figs. 2a–2c we can see that the shock wave reaches the border at ≈ 1.5 ps. This velocity of the shock wave is near the sound velocity in Au. From this the maxima would be about 3 and 4.5 ps by reflection – where with our nonreflecting boundary condition we see minima!

Acknowledgements

One of us (K.B.) enjoyed a stimulating and enlightening discussion about the temporal evolution of the impact process with Y.K. Bae, when at St. Malo. We are extremely thankful to all participants of our group at the Institute, and especially H. Barth and P. Borrmann for their helpful discussions and ideas. Also we acknowledge the RRZN at Hannover where most of simulations were computed. We praise especially Y. LeBeyec, for organizing the conference at St. Malo, and who made it possible for us to take part.

References

- [1] L. Verlet, Phys. Rev. 159 (1967) 98.
- [2] W.F. van Gusteren and H.J.C. Berendsen, in: Molecular Liquides – Dynamics and Interactions, A.J. Barnes et al., eds. (Reidel, 1984) p. 475.
- [3] B. Nitzschmann, Diploma thesis, University of Oldenburg, Germany, 1992.
- [4] H. Haberland, Z. Insepov and M. Moseler, Z. Phys. D 26 (1993) 229.
- [5] C.L. Cleveland and U. Landman, Science 257 (1992) 355.
- [6] J. Gspann, KFK Nachrichten 23, 2–3 (1991) 124.
- [7] K.H. Mueller, J. Appl. Phys. 61 (1987) 2516.
- [8] M.H. Shapiro and T.A. Tombrello, Nucl. Instr. and Meth. B 62 (1991) 35.
- [9] R.W. Hockney and J.W. Eastwood, Computer Simulation Using Particles (Hilger, Bristol, 1988) p. 278.
- [10] C.W. Gear, Report ANL 7126, Argonne National Laboratory, 1966.
- [11] M.P. Allen and D.J. Tildesley, Computer Simulation of Liquids (Clarendon, Oxford, 1987).
- [12] H.J.C. Berendsen and W.F. van Gusteren, Proc. Enrico Fermi Summer School, Varenna, Italie, 1985 p. 43.
- [13] Ch. Kittel, Einführung in die Festkörperphysik, 7th ed. (Oldenbourg Verlag, 1988).
- [14] J.D. Weinstein, R.T. Fisher, S. Vasanawala, M.H. Shapiro and T.A. Tombrello, Brown Bag Preprint Series BB-119, 1993.
- [15] M.H. Shapiro and T.A. Tombrello, Brown Bag Preprint Series BB-116; 1993.
- [16] J.D. Pelletier, M.H. Shapiro and T.A. Tombrello, Nucl. Instr. and Meth. B 67 (1991) 296.
- [17] H. Barth, Diploma thesis, University of Oldenburg, 1992.